Production of slow positron bunches using a microtron accelerator

A. P. Mills, Jr., E. D. Shaw, R. J. Chichester, and D. M. Zuckerman

AT&T Bell Laboratories, Murray Hill, New Jersey 07974

(Received 21 November 1988; accepted for publication 28 January 1989)

The microtron accelerator at Bell Laboratories presently produces 16-μs-long, 40-mA pulses of 18.5-MeV electrons at a repetition rate of 30 Hz. Energetic positron-electron pairs are produced at a 4-mm-thick W beam dump. The positrons are moderated to a few electron volts energy by a 9-mm-diam W(110) single crystal and bunched by a parabolic potential accelerator to 14-ns full width at half maximum bursts containing $(7 \pm 1) \times 10^4$ positrons. The collection efficiency of the buncher is 63%. With the buncher turned off, the positron production efficiency is 4×10^{-8} positrons per electron.

INTRODUCTION

Slow positrons may be produced by moderating to thermal energies the fast positrons from a radioactive source[1] or from a bremsstrahlung-pair production target irradiated by relativistic electrons.[2] Since the first demonstrations of feasibility,[1,2] there have been hundreds of interesting studies of positron interactions with surfaces and with atoms.[3] For many experiments it is indispensible to have a pulsed source of positrons. While it is possible to form pulses from a continuous beam,[4] intense pulses of positrons are readily obtained from an electron accelerator, as first demonstrated by Howell, Alverez, and Stanek.[5] We have made a pulsed source of slow positrons using a microtron accelerator. The comparatively long microtron pulse is compressed by three orders of magnitude using an rf trap and harmonic potential buncher.[4] We record here the details of construction and operation so that others may benefit from our experience as we have greatly benefited from descriptions of other pair production positron sources.[6–13] It is notable that whereas the electron accelerators used to date have all been LINACs, our microtron is a relatively small scale device. The positron source is at the beam dump and does not interfere with the main function of the accelerator as a producer of an electron beam for free electron laser studies.

I. MICROTRON ACCELERATOR

A microtron accelerates electrons as they pass repeatedly through a high-power microwave resonator located in a homogeneous magnetic field. In our 90-cm-diam magnet, the electrons are accelerated 25 times through a 3.00-GHz rf cavity. The rf voltage gained by the electrons is such that the return time to the rf cavity increases by one rf period with each passage. The final electron beam energy is tunable from 11 to 23 MeV by simultaneous adjustment of the rf voltage and the magnetic field. The electron beam is extracted from the accelerator through a shimmed iron tube and focused into a 10-m-long helical undulator having a 20-cm period designed for free electron laser operation at far infrared wavelengths.[14] The beam traverses the 450-G undulator field with a beam area of about 1 cm^2. The microtron produces 16-μs pulses at a 30-Hz repetition rate. The average beam current of 20-μA at 18.5 MeV is comparable to that obtainable from an rf linear accelerator, while the microtron is simpler in construction and less costly.

A plan view of the facility is shown in Fig. 1; a side view of the microtron and the undulator is shown in Fig. 2. At the end of the accelerator, the electrons are bent upwards to avoid hitting the laser mirror, and are dissipated in either a Faraday cup or the positron production target.

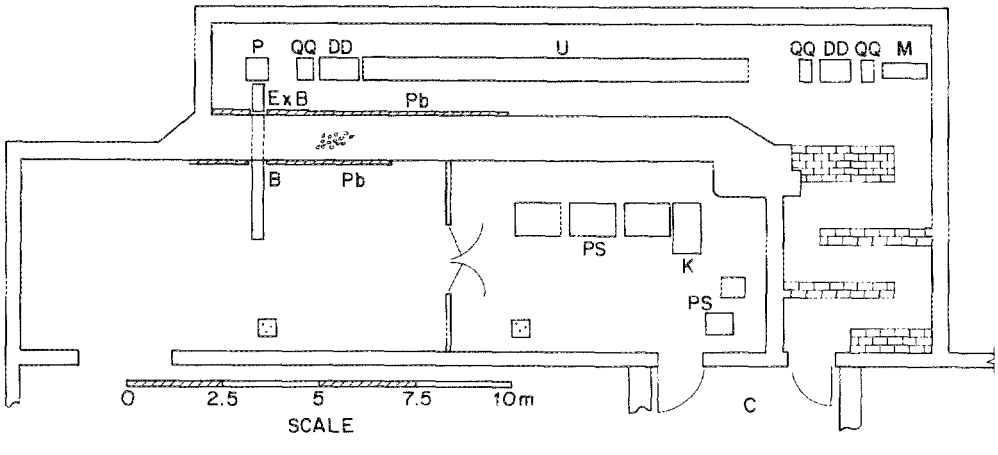

FIG. 1. Plan of the facility. *M*: microtron accelerator; *QQ*: quadrupole doublet; *D*: dipole bending magnet; *U*: helical undulator magnet; *P*: positron production target; $E \times B$: positron velocity filter; *B*: buncher; Pb: lead wall; *PS*: klystron power supplies; *K*: klystron; *C*: control room.

 0034-6748/89/050825-06$01.30 © 1989 American Institute of Physics

Downloaded 12 Sep 2005 to 138.23.236.55. Redistribution subject to AIP license or copyright, see http://rsi.aip.org/rsi/copyright.jsp

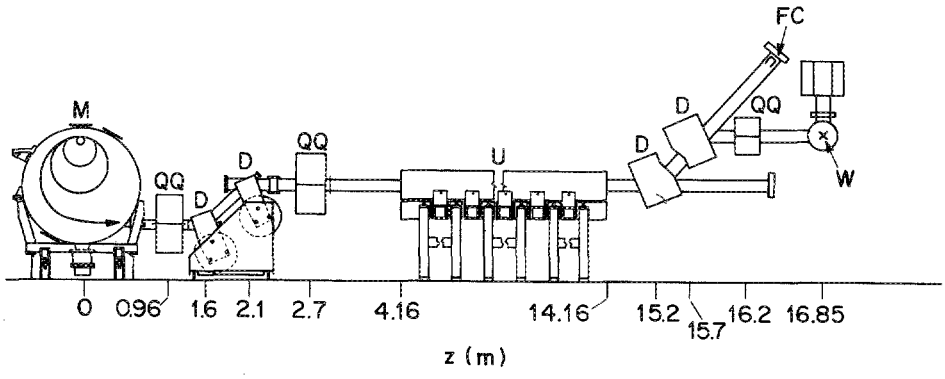

FIG. 2. Microtron accelerator, *M*, beam transport magnets, and positron production target, *W*. The magnetic elements are as follows: *QQ*: quadrupole doublet; *D*: dipole bending magnet; *U*: helical undulator magnet. When the electron beam is not being used to produce positrons, it is stopped in a Faraday cup beam dump, *FC*.

II. SLOW POSITRON SOURCE

Energetic shower positrons are produced by the interaction of the relativistic electron beam with a 3.8-mm-thick, sintered W target shown in Fig. 3. The positrons are moderated by a W(110) single crystal placed as shown for optimum efficiency. The W crystal is prepared by heating to about 2000 K *in situ*. The W target is held at ground potential, and the W crystal is biased at $+2.75$ V. As shown in Fig. 4, the slow positrons from the W crystal, guided by a 150-G magnetic induction, pass through a 12.5-mm-diam hole in a 105-mm-thick 90% W shield, are deflected by a transverse electric field through an off-axis hole through 210 mm of 90% W, are brought back to the axis of the beam pipe by a second electric field, and pass through a hole in another 210-mm-thick 90% W shield. The off-axis hole is 12.5 mm in diameter and its center is 14.7 mm from the axis of the beam pipe. The $E \times B$ deflector plates are 203 mm long and spaced 20.6 mm apart. One plate of each deflector is biased at -9.20 V, and the other is at -62.5 V. After the last shield, the positrons pass through an rf cavity, *R*, and a bunching accelerator, *B*, and, finally, hit a channel electron multiplier array detector, CEMA, that has a phosphor screen for displaying the beam profile. An image of the positron beam taken with the rf cavity and buncher turned off is shown in Fig. 5. The beam cross section, an oval approximately 7×8 mm^2, is slightly smaller than the face of the W(110) crystal. The beam spot is elongated due to passage through the $E \times B$ deflectors.

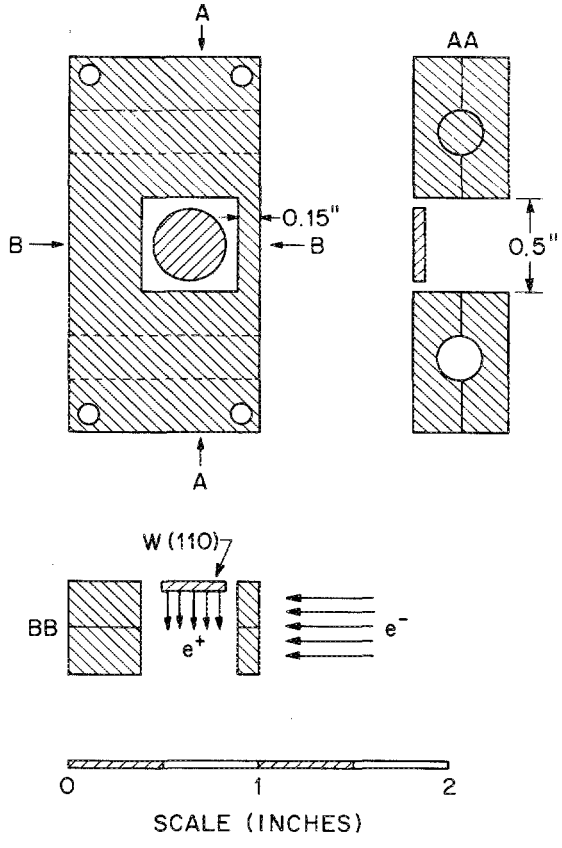

FIG. 3. Mechanical drawing of the positron production target and slow positron moderator. The electron beam impinges on a target made of sintered tungsten 0.15" = 3.8 mm thick. The target is in two halves that are clamped around two 0.25" = 6.4-mm-diam water cooling tubes made of stainless steel. The energetic shower positrons are moderated to a few electron volts energies by a W(110) single crystal that has been prepared by heating up to $\approx$2000 K *in situ*.

A Co^{58} β^+ source indicated in Fig. 4 may be positioned in front of the W(110) moderator by remote control. The source is used to test the moderator efficiency and to optimize the transmission efficiency of the positron beamline. A 3×3-in. NaI(Tl) detector located on the axis of the beam and 30 cm from the CEMA cathode measures the positron intensity. By detecting the positrons in coincidence using both the CEMA and the NaI(Tl) signals, the NaI(Tl) efficiency was determined to be $(9.0 \pm 0.5) \times 10^{-3}$ detected γ rays per positron at the CEMA.

III. BUNCHER

The relatively long pulse of slow positrons is trapped in a magnetic bottle and bunched into a short pulse using a parabolic potential accelerator.[4] The mechanical and electrical drawings for the buncher are shown in Figs. 6 and 7. The positrons are trapped after passing through the pinched magnetic field at the entrance to the magnetic bottle by a transverse rf electric field tuned to the positron cyclotron resonance. Figure 8 shows a cross section of the 430-MHz rf cavity for exciting the positron cyclotron resonance. The frequency and the $\approx$1-V amplitude of the rf driving voltage are carefully tuned for optimum trapping.

The buncher is made of 100 rings of stainless steel, 25.4 mm inside diameter. The rings are connected to two resistor

Downloaded 12 Sep 2005 to 138.23.236.55. Redistribution subject to AIP license or copyright, see http://rsi.aip.org/rsi/copyright.jsp

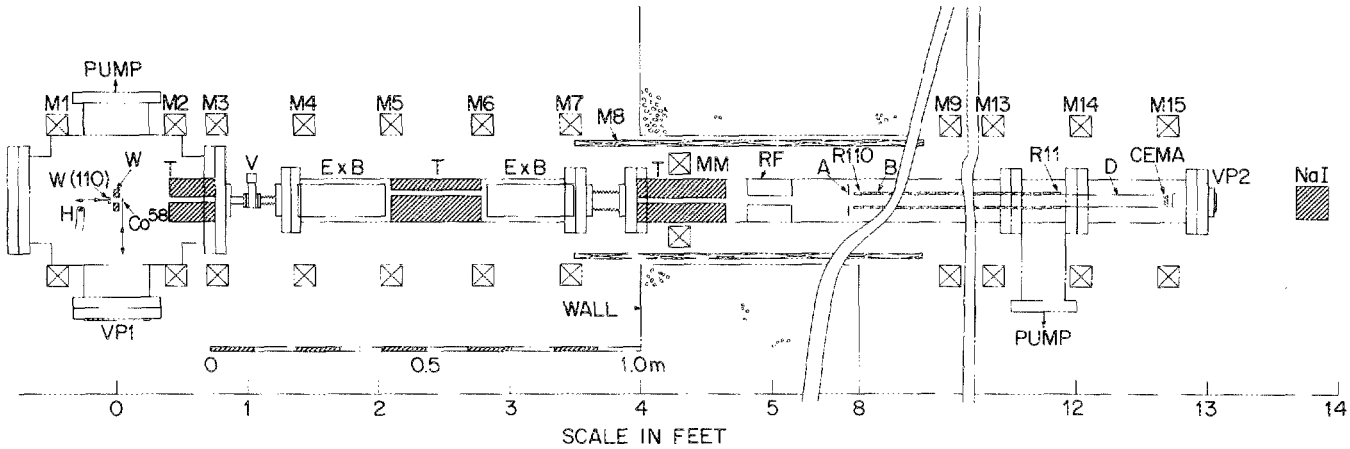

FIG. 4. Side view of the entire positron beamline: M 1–M 15: magnet coils; W: positron production target; single crystal W(110) slow positron moderator; H: electron bombardment filament for heating the crystal; retractable radioactive Co^{58} source for calibration; VP 1 and VP 2: viewports; T: 90% tungsten alloy shielding cylinders; V: pneumatic valve; $E \times B$ deflectors; MM: magnetic mirror coil; RF: rf resonator cavity; A: grounded aperture; B: parabolic potential buncher consisting of accelerator rings R 11–R 110; D: drift tube; CEMA: channel plate detector; and 3×3-in. NaI(Tl) detector. Not shown are 6–8 in. of Pb blocks on each side of the 4-foot-thick concrete wall, quantities of Pb surrounding the $E \times B$ section, bags of Pb shot stuffed inside coil M 8, and a 4-in.-thick Pb wall between M 9 and M 10.

chains. The first 39 are connected to a high impedance divider chain that approximates the potentials at positions $i = 11$–49 of a series $V_i = \text{const} \times i^2$. Ring number 49 is operated at about +15 V to repel the positrons prior to the bunch pulse. Ring number 11 and a drift tube attached to it are biased at a negative potential V_{11}. Rings 50–110 are connected to a 50-Ω attenuator that continues the sequence $V_i = \text{const} \times i^2$. The series resistors are ~20-mm lengths of resistance wire of varying diameter. The parallel resistors are commercial film resistors sealed in glass. When a 5-ns 10%–90% rise time pulse is applied to ring number 110, the delay before it reaches ring number 54 is 16.6 ns. The delay is four times longer than that due to the velocity of light principally because of the ≈50 nH inductance of each series resistor. To

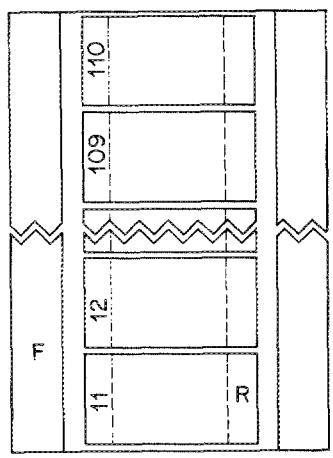

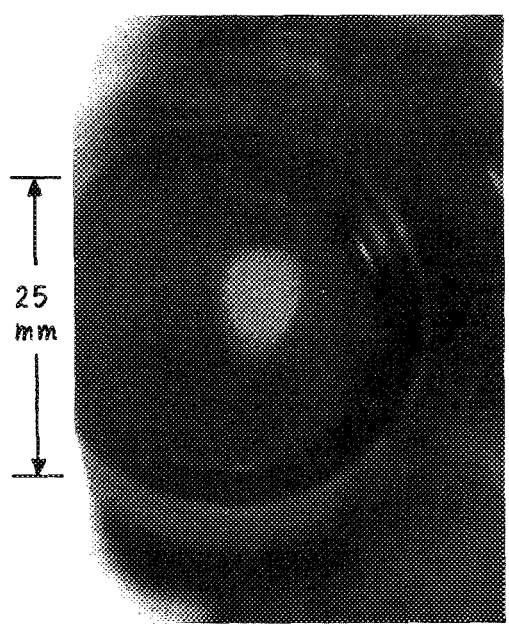

FIG. 5. Image of the positron beam on a channel plate. The phosphor screen is 25 mm in diameter.

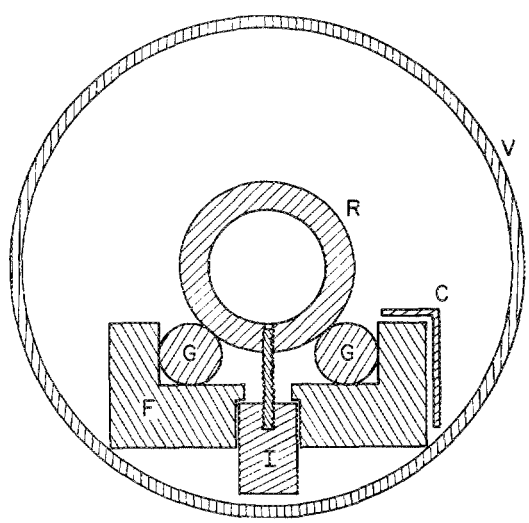

FIG. 6. Mechanical drawing of the parabolic potential buncher. V: 4-in. outside diameter vacuum chamber; R: 304 stainless-steel accelerator ring, 1.00-in. inside diameter, 1.375-in. outside diameter; C: mica dielectric capacitor plate; G: 0.500-in. diam quartz insulator rods; F: 304 stainless-steel frame; I: ceramic insulator holding ring in place. There are 100 rings R, but they start at number 11 because we are not bothering to shape carefully the first part of the parabola.

Downloaded 12 Sep 2005 to 138.23.236.55. Redistribution subject to AIP license or copyright, see http://rsi.aip.org/rsi/copyright.jsp

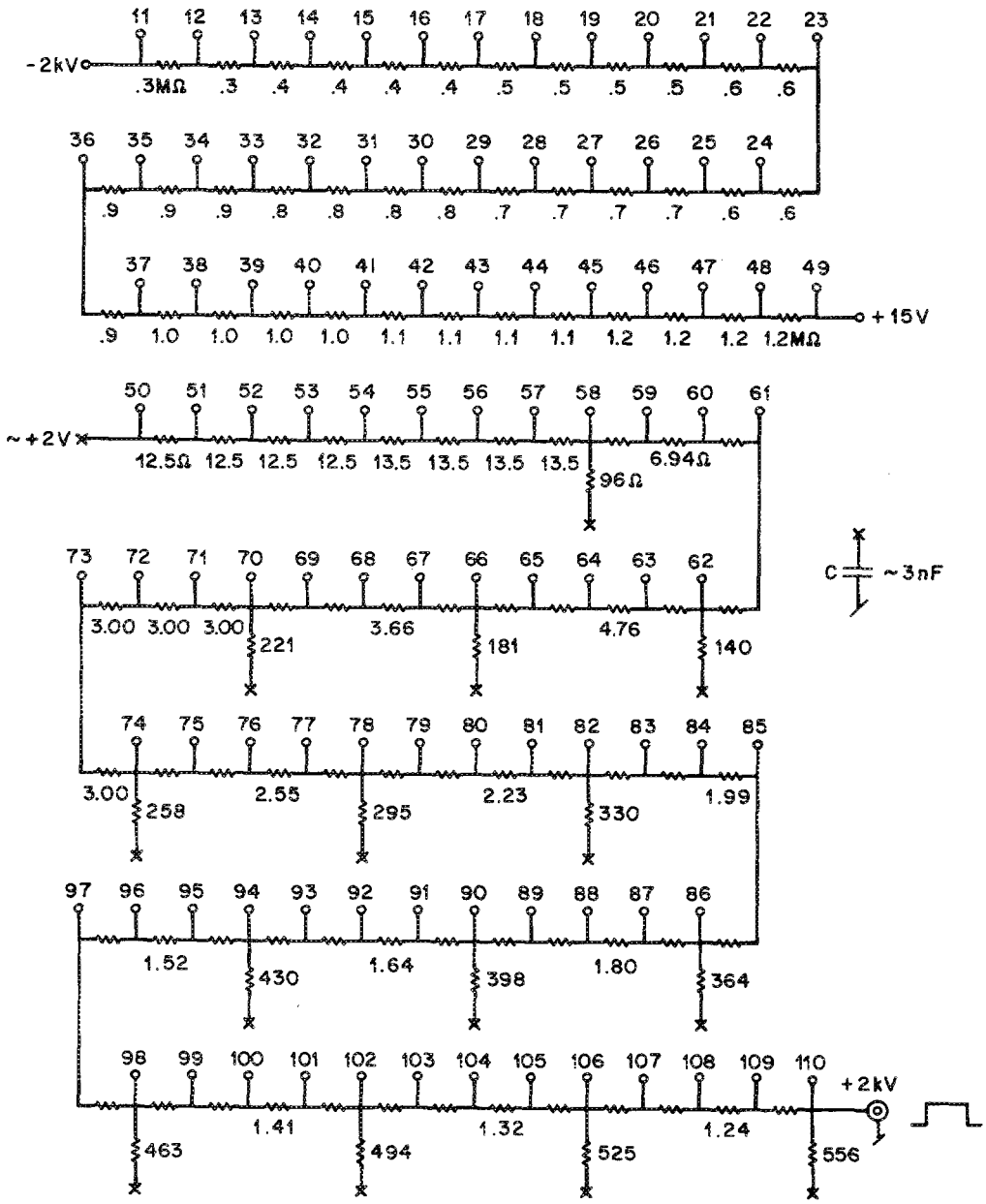

FIG. 7. Electrical circuit of the parabolic potential attenuator that comprises the buncher. The numbers refer to the 100 accelerator rings of Fig. 6.

partly compensate for the slow buncher, V_{11} is made much larger (2 kV) than its ideal value. We plan to replace the wires with low inductance film resistors, eventually. At ring number 54 the rise time of the accelerator network is about 6 ns with $\pm$ 10% overshoot. The high voltage pulser for the buncher is a thyratron circuit (Fig. 9) similar to that of Ref. 15, except that a zener diode across the avalanch transistor has been found to improve the pulse shape considerably.

RESULTS

Figure 10(a) shows the electron beam current versus time as measured by a Faraday cup at the beam dump of the free electron laser with the microtron operating at 18.5 MeV

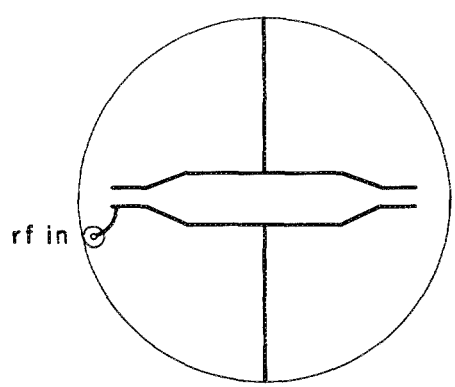

FIG. 8. Cross section of the 430-MHz rf cavity. The cavity slides into the inside of the 4-in. outside diameter vacuum pipe of Fig. 6, and is 4 in. long.

Downloaded 12 Sep 2005 to 138.23.236.55. Redistribution subject to AIP license or copyright, see http://rsi.aip.org/rsi/copyright.jsp

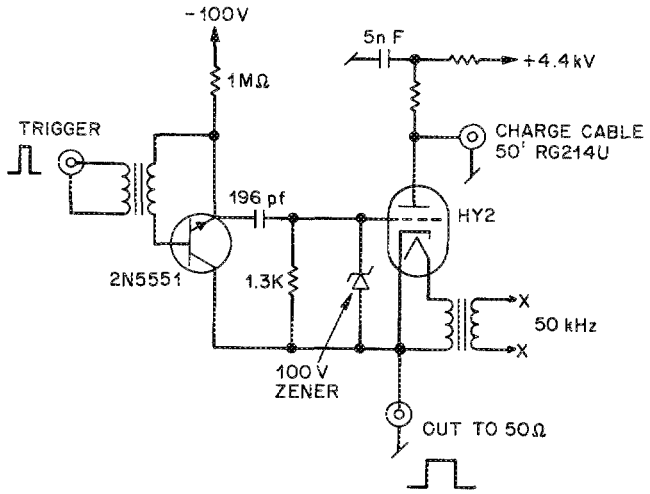

FIG. 9. Schematic of the thyratron circuit for pulsing the buncher of Fig. 7.

and at a 30-Hz repetition rate. At the end of the electron pulse, the high voltage pulse [Fig. 10(b)] is applied to the parabolic attenuator accelerator to bunch the positrons. About 100 ns later the positrons arrive at the channel electron multiplier array target with a time distribution shown in Fig. 10(c), measured with a 19-mm-diam by 19-mm-long Pilot U scintillator coupled to a Hamamatsu 1564U tube. A signal-averaging 125-MHz LeCroy transient recorder oscilloscope was used to obtain Figs. 10(b) and 10(c). The positron pulse width is 14-ns full width at half maximum (fwhm). The response time of the detector, 3.7-ns fwhm, is negligible in comparison. The 3×3-in. NaI(Tl) detector gave pulses of 400 mV into 50 Ω, compared with the 1.0-mV 511-keV photopeak amplitude measured with a small source of Na^{22} under otherwise similar conditions. The average pulse height per detected 511-keV γ ray is 68% of the photopeak height. Including all factors, we find that the pulse in Fig. 7(c) contains 72 000 positrons, with an estimated uncertainty of about 15%. Turning off the buncher, we find that the trapping efficiency is 63%, and, thus, the total positron yield per 16-μs pulse is 1.2×10^5. The slow positron production efficiency is 4×10^{-8} per 18.5-MeV electron, and the positron current is $3\times10^6\ s^{-1}$.

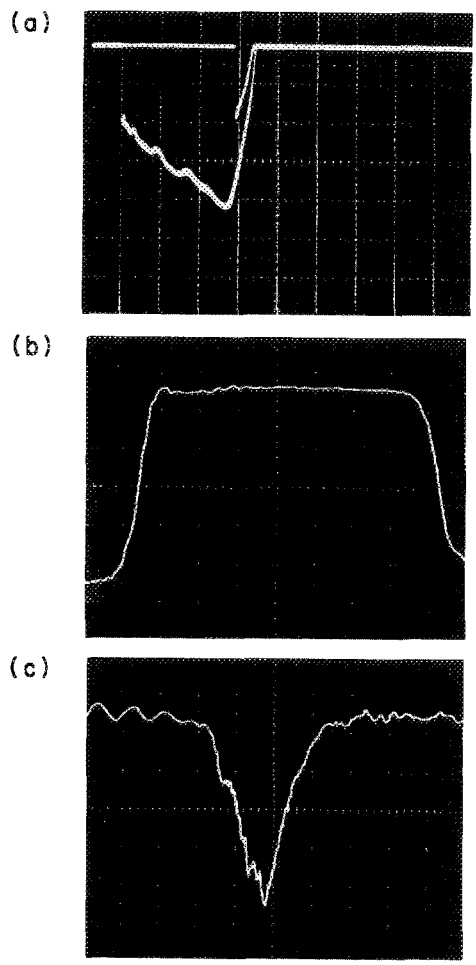

FIG. 10. (a) Electron current versus time; 5 μs and 10 mA per large division. (b) Pulse applied to the parabolic buncher; 20 ns and 400 V per division. (c) Pulse from the plastic scintillator; 10 ns and $\approx$100 mV per division.

V. COMPARISON WITH OTHER POSITRON SOURCES

Although our positron production efficiency is as good as any reported at the same energy, as can be seen from Fig. 2 of Ref. 7, our total positron beam current is one thousand times less than has been obtained by Howell and collaborators[5] using a 100-MeV LINAC operating at 1440 Hz. Our positron bunches are also presently a factor of 10 smaller than reported by Howell *et al.*[5] Nevertheless, the bunches are 10^3 times larger than we have employed in earlier experiments,[16] and we expect they will be very useful.

VI. POSSIBLE IMPROVEMENTS

We have found that when the microtron is operated at 23.2 MeV, the positron production efficiency is improved by as much as four times, although the electron current is down by an order of magnitude. It is interesting that a change in the microtron rf cavity could allow operation over a narrow range of energies around 25 MeV with no loss in operating current.[17] The microtron beamline vacuum is being improved to allow high current operation at 20.8 MeV, where we might expect to double our present efficiency. We are also expecting to be able to make the electron pulse more constant in time and, thereby, to obtain a factor of 2 increase in the total electron current. Finally, the microtron is presently being pulsed at 30 Hz, but the power supplied should allow 120 Hz. Thus, without changing the rf cavity, the total positron yield could be increased to 3×10^5 per few nanoseconds pulse and we might obtain a cw beam strength of about $5\times10^7\ e^+\ s^{-1}$ in 16-μs pulses. At 25 MeV we might hope to obtain pulses of 10^6 positrons.

ACKNOWLEDGMENTS

The authors are grateful to S. Chu, H. Enge, R. H. Howell, and H. Schneider for helpful conversations.

Downloaded 12 Sep 2005 to 138.23.236.55. Redistribution subject to AIP license or copyright, see http://rsi.aip.org/rsi/copyright.jsp

[1]W. Cherry, Ph.D. Thesis, Princeton University (1958), available from University Microfilms Inc., Ann Arbor, MI 48109, USA.
[2]D. G. Costello, D. E. Groce, D. F. Herring, and J. W. McGowan, Phys. Rev. B **4**, 1433 (1972).
[3]See, for example, A. P. Mills, Jr., in *Positron Solid State Physics*, edited by W. Brandt and A. Dupasquier (North-Holland, Amsterdam, 1983), p. 432; K. G. Lynn, *ibid.*, p. 609; P. J. Schultz and K. G. Lynn, Rev. Mod. Phys. **60**, 701 (1988)
[4]A. P. Mills, Jr., Appl. Phys. **22**, 273 (1980).
[5]R. H. Howell, R. A. Alvarez, and M. Stanek, Appl. Phys. Lett. **40**, 751 (1982).
[6]R. H. Howell, R. A. Alvarez, K. A. Woodle, S. Dhawan, P. O. Egan, V. W. Hughes, and M. W. Ritter, IEEE Trans. Nucl. Sci. **NS-30**, 1438 (1983).
[7]R. H. Howell, I. J. Rosenberg, and M. J. Fluss, Appl. Phys. A **43**, 247 (1987).
[8]G. Graff, R. Ley, A. Osipowicz, G. Werth, and J. Ahrens, Appl. Phys. A **33**, 59 (1984).
[9]R. H. Howell, I. J. Rosenberg, and M. J. Fluss, Appl. Phys. A **43**, 247 (1987).
[10]M. Dorikens, L. Dorikens-Vanpraet, D. Segers, and I. Lemahieu, Appl. Phys. A **43**, 257 (1987).
[11]J. Dahm, K. D. Niebling, R. Ley, and G. Werth, Appl. Phys. A **44**, 105 (1987).
[12]F. Ebel, W. Faust, C. Hahn, S. Langer, and H. Schneider, Appl. Phys. A **44**, 119 (1987).
[13]L. D. Hulett, Jr., T. A. Lewis, R. G. Alsmiller, Jr., R. Peelle, S. Pendyala, J. M. Dale, and T. M. Rosseel, Nucl. Instrum. Methods Phys. Res. B **24/25**, 905 (1987).
[14]E. D. Shaw, R. J. Chichester, and S. C. Chen, Nucl. Instrum. Methods Phys. Res. A **250**, 44 (1986).
[15]A. P. Mills, Jr., in *Positron Scattering in Gases*, edited by J. W. Humberston and M. R. C. McDowell (Plenum, New York, 1983), p. 121.
[16]See, for example, S. Chu and A. P. Mills, Jr., Phys. Rev. Lett. **48**, 1333 (1982); and A. P. Mills, Jr., L. Pfeiffer, and P. M. Platzman, Phys. Rev. Lett. **51**, 1085 (1983).
[17]According to S. P. Kapitza and V. N. Melekhin, [*The Microtron*, translated from the Russian by I. N. Sviatoslavsky and edited by Ednor M. Rowe (Harwood, London, 1978), p. 11] the rf energy may be coupled to the electron beam of a microtron in two ways. At present our microtron has a type 1 rf cavity that allows an energy gain per passage through the cavity, $\Omega = \Delta E / m_e c^2$, in the range $0.65 < \Omega < 1.7$. A type 2 configuration of the rf cavity gives $1.7 < \Omega < 2.2$. See also U. Bizzarri *et al.*, Nucl. Instrum. Methods Phys. Res. A **250**, 254 (1986).

Downloaded 12 Sep 2005 to 138.23.236.55. Redistribution subject to AIP license or copyright, see http://rsi.aip.org/rsi/copyright.jsp